Research Article

Analysis of Laser Pulse Heating Model Using the Finite Element Analysis

Erhuvwuvoke EBOJOH[1*], John Ajokpaoghene AKPOBI[2], Kelechi NWOSU[2]

[1]University of Benin, Faculty of Engineering, Department of Production Engineering, Benin City, Nigeria
[2]University of Benin, P.M.B 1154 Benin City, Nigeria

*Corresponding Author: voke.ebojoh@uniben.edu
ORCID: 0000-0001-5432-6020

Abstract:

The Model equation for the laser heating process is a two dimensional partial differential equation in cylindrical coordinate that is time dependent and involves a source term. This work presents a sequential method in obtaining solution to the laser heat equation using a unique method of solution known as Finite Element Method; a numerical approach as against the analytical method. The approach was used in analyzing the temperature of the irradiated material within the domain of the material. This was done by multiplying the model differential equation by a weighted function and carrying out integration over the domain of the problem to obtain the weak form of the equation. Triangular and rectangular Langrage interpolation functions were used for the spatial discretization and Alpha family of approximation was used for the time approximation. The domain of the problem was discretized manually using eight triangular and 4 rectangular finite element mesh. To obtain more accurate solutions, a programme written with MATLAB software was used to further discretize the domain into smaller finite elements (4000 triangular element mesh and 2000 rectangular element mesh). The results obtained was plotted and compared with literature.

1. Introduction

The Finite Element Method (FEM) (Sometimes referred to as Finite Element Analysis (FEA) is a numerical technique for finding approximate solution to partial differential equation (PDE), ordinary differential equation (ODE) as well as integral equations. This solution approach is based on either eliminating the differential equation completely (steady state problem), or rendering the PDE into an approximating system of ordinary differential equation, which are then numerically integrated using standard techniques. The concept of Finite element is well treated in many standard texts [1] and [2].As a result of the complexity and relative longer time to obtain analytical solution to several engineering model partial differential equation being developed by various researchers,

approximate method of solutions (such as Finite difference and Finite Element) are often used for such analysis. Also to aid the computation some commercially developed Finite Element software like ANSYS, ADINA, Abaqus, GetFEM++, VisualFEA, JMAG, Nastran, Mecway are also used for analysis as well as to carry out simulations. Finite Element Method of numerical solution have been used to solve various engineering problems, [3] used finite element to analyze the distribution of velocity in viscous incompressible fluid flow using Lagrange interpolation function. Reference [4] investigated the Boussinesq-type flow model for non linear dispersive wave. They used Finite element discretization technique in their analysis of the wave equation.

Reference [5] Investigated numerically the mixed convection heat transfer through a vertical wavy isothermal channels the governing equations consisting of continuity, momentum and energy equations were solved numerically by finite element method using Characteristic Based Split (CBS) algorithm, the effect of Reynolds, Prandtl and Grashof numbers on flow and thermal fields were also investigated. Reference [6] used finite element method to analyze convective heat transfer in a porous medium. This method was used to analyze the convection in vertical surface embedded in the medium and convection in a confined porous medium enclosure. Considerable research studies have been carried out to explore heating and machining processes. Reference [7] gave an overview of the state of the art laser beam machining in general with special emphasis on applications of short and ultra-short lasers. The research showed that in micro-machining, shorter pulses reduce heat-affected damage of the material and opens new ways for nanometer accuracy. Reference [8] examined the laser thermal stresses during the laser drilling process. Other works on laser beam machining include those of [9]–[13].

Reference [14] used a numerical solution to analyze the partial differential heat equation. They examined the cavity depth and formations in the irradiated steel. Also [15] used Laplace transformation method to obtain an analytical solution for laser short pulse heating due to evaporative boundary condition. In this paper the laser heat equation is solved using both rectangular and triangular Finite Element discretization. A program written with MATLAB was used to increase the number of elements used for the discretization and to decrease the time step which consequently produced very accurate solution relative to the manual discretization.

2. Methodology

The governing equation being solved is the heat equation in cylindrical coordinate with an exponential source term (the Laser pulse), given as;

$$\rho c_p \frac{\partial T}{\partial t} = \frac{k}{r}\frac{\partial}{\partial r}\left(r\frac{dT}{dr}\right) + k\frac{\partial^2 T}{\partial z^2} + \left(I_o \delta(1-r_f)\exp(-\delta z)\exp\left(-\frac{r^2}{a^2}\right)\right) \quad (1)$$

Where c_p = Specific heat capacity, k = Thermal conductivity δ = absorption coefficient ρ = density, r_f = reflectivity I_0 = laser peak power intensity a = Gaussian parameter

conditions are as follows;

Initial condition at time $t = 0$

$$t = 0 \rightarrow T(r,z,0) = T_O \quad (2)$$

At the boundary,

$$z = b \rightarrow T(r,b,t) = T_O \quad (3)$$

$$r = a \rightarrow T(a,z,t) = T_O \quad (4)$$

From Symmetry

At position $r = 0 \rightarrow \dfrac{\partial T(0,z,t)}{\partial r} = 0$

At the surface where $z = 0 \rightarrow \dfrac{\partial T(r,0,t)}{\partial z} = 0 \quad (5)$

To obtain the weak form of (1), we multiply (1) by a weight function V and integrate over the domain

$$0 = \int_\Omega \left[\left(\rho c_p \frac{\partial T}{\partial t}\right) - V\frac{k}{r}\frac{\partial}{\partial r}\left(r\frac{dT}{dr}\right) - Vk\frac{\partial^2 T}{\partial z^2} - V\left(I_o\delta(1-r_f)\exp(-\delta z)\exp\left(-\frac{r^2}{a^2}\right)\right)\right] r dr dz \quad (6)$$

Representing $\left(I_o\delta(1-r_f)\exp(-\delta z)\exp\left(-\frac{r^2}{a^2}\right)\right) \quad (7)$

as f and carrying out integration by parts our week form becomes;

$$0 = \int_\Omega \left[Vr\left(\rho c_p \frac{\partial T}{\partial t} - Vf\right) + k\frac{\partial V}{\partial r}\left(r\frac{dT}{dr}\right) + k\frac{\partial V}{\partial z}r\frac{\partial T}{\partial z}\right]drdz - \iint_r q_n V ds \quad (8)$$

where $q_n = r\frac{\partial T}{\partial r}n_r + r\frac{\partial T}{\partial z}n_z \quad (9)$

To obtain the Finite Element model, we assume an approximation solution for an element "e" of the form;

$$T(r,z,t) = \sum_{j=1}^{n} \left(T_j^e(t)\psi_j^e(r,z) \right)$$

(10)

The semi discrete finite element model is obtained by substituting the finite element approximation for the dependent variable T and substituting V for ψ_i, where ψ is the Lagrange interpolation function for a two dimensional differential equation.

We have the equation in Matrix form as;

$$\left[M_{ij}^e \right] \left\{ \dot{T}_j^e \right\} + \left[K_{ij}^e \right] \left\{ T_j^e \right\} = \left\{ F_i^e \right\} + \left\{ Q_i^e \right\}$$

(11)

Where functions enclosed in square brackets and curly brackets are square and column matrix respectively.

Also,

$$\frac{dT}{dt} = \dot{T}$$

(12)

$$M_{ij}^e = \int_{zaa}^{zaa+b} \int_{zaa}^{zaa+b} \left(\rho c_p r \psi_i \psi_j \right) \, drdz$$

(13)

$$K_{ij}^e = \int_{zaa}^{zaa+b} \int_{raa}^{raa+a} k \left(r \frac{d\psi_i}{dr} \frac{d\psi_j}{dr} + r \frac{d\psi_i}{dz} \frac{d\psi_j}{dz} \right) drdz$$

(14)

$$f_i^e = \int_{zaa}^{zaa+b} \int_{raa}^{raa+a} \left(r\psi_i \left(I_o \delta \left(1 - r_f \right) \exp\left(-\delta z \right) \exp\left(-\frac{r^2}{a^2} \right) \right) \right) drdz$$

(15)

The coefficient matrix for M_{ij}^e, K_{ij}^e and f_i^e are evaluated from (13), (14) and (15);

Where for the rectangle interpolation, i and j takes values of 1, 2, 3 and 4

And for the triangular interpolation, i and j takes values of 1, 2 and 3.

The results of the integration are shown in matrix form, using the rectangular interpolation functions

$$M_{ij}^e = \rho c_p \begin{bmatrix} \frac{(ab(a+4raa))}{36} & \frac{(ab(a+2raa))}{36} & \frac{(ab(a+2raa))}{72} & \frac{(ab(a+4raa))}{72} \\ \frac{(ab(a+2raa))}{36} & \frac{(ab(3a+4raa))}{36} & \frac{(ab(3a+4raa))}{72} & \frac{(ab(a+2raa))}{72} \\ \frac{(ab(a+2raa))}{72} & \frac{(ab(3a+4raa))}{72} & \frac{(ab(3a+4raa))}{36} & \frac{(ab(a+2raa))}{36} \\ \frac{(ab(a+4raa))}{72} & \frac{(ab(a+2raa))}{72} & \frac{(ab(a+2raa))}{36} & \frac{(ab(a+4raa))}{36} \end{bmatrix}$$

(16)

Using triangular interpolation function we obtain;

$$M_{ij}^e = \frac{ab\rho c_p}{12} \begin{bmatrix} (a+4raa) & -raa & (a+3raa) \\ -raa & (a+2raa) & -raa \\ (a+3raa) & -raa & (2(a+2raa)) \end{bmatrix}$$

(17)

Also for rectangular interpolation function; Due to the presence of the exponential function, the f_i^e coefficient matrix would be evaluated numerically. Fig. 1 and 2 shows the local nodes (node1, node2, node3 and node4) four each of the four rectangular elements and the local nodes (node 1, node 2, and node 3) four each of the eight triangular elements that make up the domain respectively, as well as the global nodes when assembled (node1, node2, ..., node8 and node9).fter inputting boundary condition the assembled equation using Rectangular Lagrange interpolation function we have and for the triangular interpolation function

$$K_{ij}^e = k \begin{bmatrix} \left[\dfrac{b\left(\frac{a}{6}+\frac{raa}{3}\right)}{a}+\dfrac{\left(\frac{a^3}{12}+\frac{raa\cdot a^2}{3}\right)}{ab}\right] & \dfrac{\left(a^2-2b^2\right)\left(a+2raa\right)}{12ab} & -\dfrac{\left(a^2+b^2\right)\left(a+2raa\right)}{12ab} & \left[\dfrac{b\left(\frac{a}{12}+\frac{raa}{6}\right)}{a}-\dfrac{\left(\frac{a^3}{12}+\frac{raa\cdot a^2}{3}\right)}{ab}\right] \\[4ex] \dfrac{\left(a^2-2b^2\right)\left(a+2raa\right)}{12ab} & \left[\dfrac{b\left(\frac{a}{6}+\frac{raa}{3}\right)}{a}+\dfrac{\left(\frac{a^3}{4}+\frac{raa\cdot a^2}{3}\right)}{ab}\right] & \left[\dfrac{b\left(\frac{a}{12}+\frac{raa}{6}\right)}{a}-\dfrac{\left(\frac{a^3}{4}+\frac{raa\cdot a^2}{3}\right)}{ab}\right] & -\dfrac{\left(a^2+b^2\right)\left(a+2raa\right)}{12ab} \\[4ex] -\dfrac{\left(a^2+b^2\right)\left(a+2raa\right)}{12ab} & \left[\dfrac{b\left(\frac{a}{12}+\frac{raa}{6}\right)}{a}+\dfrac{\left(\frac{a^3}{4}+\frac{raa\cdot a^2}{3}\right)}{ab}\right] & \left[\dfrac{b\left(\frac{a}{6}+\frac{raa}{3}\right)}{a}+\dfrac{\left(\frac{a^3}{4}+\frac{raa\cdot a^2}{3}\right)}{ab}\right] & \dfrac{\left(a^2-2b^2\right)\left(a+2raa\right)}{12ab} \\[4ex] \left[\dfrac{b\left(\frac{a}{12}+\frac{raa}{6}\right)}{a}-\dfrac{\left(\frac{a^3}{12}+\frac{raa\cdot a^2}{3}\right)}{ab}\right] & -\dfrac{\left(a^2+b^2\right)\left(a+2raa\right)}{12ab} & \dfrac{\left(a^2-2b^2\right)\left(a+2raa\right)}{12ab} & \left[\dfrac{b\left(\frac{a}{6}+\frac{raa}{3}\right)}{a}+\dfrac{\left(\frac{a^3}{12}+\frac{raa\cdot a^2}{3}\right)}{ab}\right] \end{bmatrix} \quad (18)$$

$$K_{ij}^e = k \begin{bmatrix} \dfrac{b\left(a+2raa\right)}{2a} & \dfrac{-b\left(a+2raa\right)}{2a} & 0 \\[3ex] \dfrac{-b\left(a+2raa\right)}{2a} & \dfrac{\left(\left(a^2+b^2\right)\left(a+2raa\right)\right)}{2ab} & \dfrac{-a\left(a+2raa\right)}{2b} \\[3ex] 0 & \dfrac{-a\left(a+2raa\right)}{2b} & \dfrac{a\left(a+2raa\right)}{2b} \end{bmatrix} \quad (19)$$
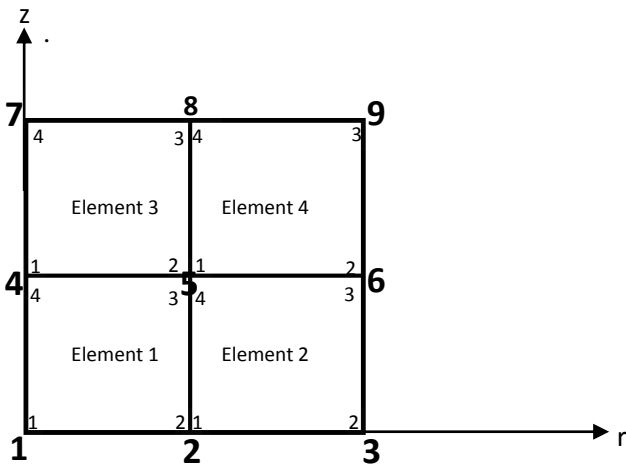

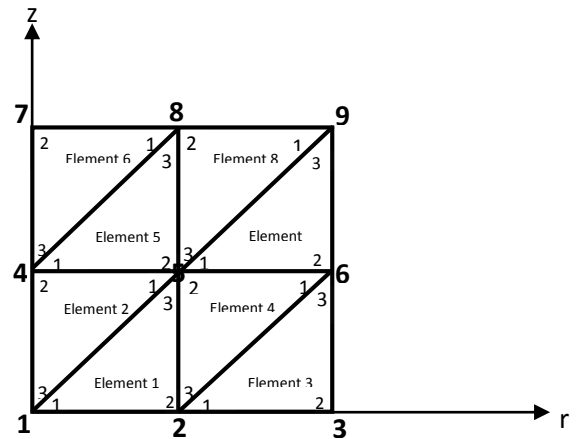**Fig. 1:** *Four rectangular element mesh showing positions*

Fig. 2: *Eight triangular element mesh showing nodal positions*

:

$$\begin{bmatrix} K_{11}^1 & K_{12}^1 & K_{14}^1 & K_{13}^1 \\ K_{21}^1 & \left(K_{22}^1+K_{11}^1\right) & K_{24}^1 & \left(K_{23}^1+K_{14}^2\right) \\ K_{41}^1 & K_{42}^1 & \left(K_{44}^1+K_{11}^3\right) & \left(K_{43}^1+K_{12}^3\right) \\ K_{31}^1 & \left(K_{32}^1+K_{41}^2\right) & \left(K_{34}^1+K_{21}^3\right) & \left(K_{33}^1+K_{44}^2+K_{22}^3+K_{11}^4\right) \end{bmatrix} \begin{Bmatrix} T_1 \\ T_2 \\ T_4 \\ T_5 \end{Bmatrix}$$

$$
+ \begin{bmatrix} M_{11}^1 & M_{12}^1 & M_{14}^1 & M_{13}^1 \\ M_{21}^1 & \left(M_{22}^1 + M_{11}^1\right) & M_{24}^1 & \left(M_{23}^1 + M_{14}^2\right) \\ M_{41}^1 & M_{42}^1 & \left(M_{44}^1 + M_{11}^3\right) & \left(M_{43}^1 + M_{12}^3\right) \\ M_{31}^1 & \left(M_{32}^1 + M_{41}^2\right) & \left(M_{34}^1 + M_{21}^3\right) & \left(M_{33}^1 + M_{44}^2 + M_{22}^3 + M_{11}^4\right) \end{bmatrix} \begin{Bmatrix} \dot{T_1} \\ \dot{T_2} \\ \dot{T_4} \\ \dot{T_5} \end{Bmatrix} = \begin{Bmatrix} FF_1^1 \\ FF_2^1 + FF_1^2 \\ FF_4^1 + F_1^3 \\ FF_3^1 + FF_4^2 + FF_2^3 + FF_1^4 \end{Bmatrix}
$$

(20)

Where;

$$
\begin{Bmatrix} FF_1^1 \\ FF_2^1 + FF_1^2 \\ FF_4^1 + FF_1^3 \\ FF_3^1 + FF_4^2 + FF_2^3 + FF_1^4 \end{Bmatrix} = \begin{Bmatrix} F_1^1 \\ F_2^1 + F_1^2 \\ F_4^1 + F_1^3 \\ F_3^1 + F_4^2 + F_2^3 + F_1^4 \end{Bmatrix} - \begin{bmatrix} 0 & 0 & 0 & 0 & 0 \\ K_{12}^2 & K_{13}^2 & 0 & 0 & 0 \\ 0 & 0 & K_{14}^3 & K_{13}^3 & 0 \\ K_{42}^2 & \left(K_{43}^2 + K_{12}^4\right) & K_{24}^3 & \left(K_{23}^3 + K_{14}^4\right) & K_{13}^4 \end{bmatrix} \begin{bmatrix} T_o \\ T_o \\ T_o \\ T_o \\ T_o \end{bmatrix}
$$

$$
- \begin{bmatrix} 0 & 0 & 0 & 0 & 0 \\ M_{12}^2 & M_{13}^2 & 0 & 0 & 0 \\ 0 & 0 & M_{14}^3 & M_{13}^3 & 0 \\ M_{42}^2 & \left(M_{43}^2 + M_{12}^4\right) & M_{24}^3 & \left(M_{23}^3 + M_{14}^4\right) & M_{13}^4 \end{bmatrix} \begin{bmatrix} T_o \\ T_o \\ T_o \\ T_o \\ T_o \end{bmatrix}
$$

(21)

And the assembled equation using Triangular Lagrange interpolation function is:

$$
\begin{bmatrix} \left(K_{11}^1 + K_{33}^2\right) & K_{12}^1 & K_{22}^2 & \left(K_{13}^1 + K_{31}^2\right) \\ K_{21}^1 & \left(K_{22}^1 + K_{11}^3 + K_{33}^4\right) & 0 & \left(K_{23}^1 + K_{32}^4\right) \\ K_{23}^2 & 0 & \left(K_{22}^2 + K_{11}^5 + K_{33}^6\right) & \left(K_{23}^2 + K_{12}^5\right) \\ \left(K_{31}^1 + K_{13}^2\right) & \left(K_{32}^1 + K_{23}^4\right) & \left(K_{12}^2 + K_{21}^5\right) & \left(K_{33}^1 + K_{11}^2 + K_{22}^5 + K_{11}^7 + K_{33}^8\right) \end{bmatrix} \begin{Bmatrix} T_1 \\ T_2 \\ T_4 \\ T_5 \end{Bmatrix}
$$

$$
+ \begin{bmatrix} \left(M_{11}^1 + M\right)_{3\,3} & M^1_{1\,2} & M^2_{3\,2} & \left(+ M^1\right) M^2_{3} \\ M^1_{2\,1} & \left(M^1_{2\,2} M^3_{\,1}\right) M^4_{3\,0} & & \left(+ M^1\right) M^4_{3} \\ M^2_{2\,3} & 0 & \left(M^2_{2\,2} M^5_{\,1}\right) M^6_{3\,3} & \left(+ M^2\right) M^5_{1} \\ \left(M^1_{3\,1} M\right)_{1\,3} & \left(M^1_{\,3}\right) M^4 & \left(_3 + M^5\right) & M^4_{\,2} + _2 M^1 + M^2_{\,3} M^4 + M \end{bmatrix} \begin{Bmatrix} \dot{T_1} \\ \dot{T_2} \\ \dot{T_4} \\ \dot{T_5} \end{Bmatrix} = \begin{Bmatrix} FF_1^1 + FF_3^2 \\ FF_1^1 + FF_3^3 + FF_4^4 \\ FF_2^2 + FF_1^5 + FF_3^6 \\ FF_3^1 + FF_1^2 + FF_2^4 + FF_2^5 + FF_1^7 + FF_3^8 \end{Bmatrix}
$$

(22)

Where;

$$
\begin{Bmatrix} FF_1^1 + FF_3^2 \\ FF_2^1 + FF_1^3 + FF_3^4 \\ FF_2^2 + FF_1^5 + FF_3^6 \\ FF_3^1 + FF_1^2 + FF_2^4 + FF_2^5 + FF_1^7 + FF_3^8 \end{Bmatrix} = \begin{Bmatrix} F_1^1 + F_3^2 \\ F_2^1 + F_1^3 + F_3^4 \\ F_2^2 + F_1^5 + F_3^6 \\ F_3^1 + F_1^2 + F_2^4 + F_2^5 + F_1^7 + F_3^8 \end{Bmatrix} - \begin{bmatrix} 0 & 0 & 0 & 0 & 0 \\ K_{12}^3 & \left(K_{13}^3 + K_{31}^4\right) & 0 & 0 & 0 \\ 0 & 0 & K_{32}^6 & \left(K_{13}^5 + K_{31}^6\right) & 0 \\ 0 & \left(K_{21}^4 + K_{12}^7\right) & 0 & \left(K_{23}^5 + K_{32}^8\right) & \left(K_{13}^7 + K_{31}^8\right) \end{bmatrix} \begin{bmatrix} T_o \\ T_o \\ T_o \\ T_o \\ T_o \end{bmatrix}
$$

$$
- \begin{bmatrix} 0 & 0 & 0 & 0 & 0 \\ M_{12}^3 & \left(M_{13}^3 + M_{31}^4\right) & 0 & 0 & 0 \\ 0 & 0 & M_{32}^6 & \left(M_{13}^5 + M_{31}^6\right) & 0 \\ 0 & \left(M_{21}^4 + M_{12}^7\right) & 0 & \left(M_{23}^5 + M_{32}^8\right) & \left(M_{13}^7 + M_{31}^8\right) \end{bmatrix} \begin{bmatrix} T_o \\ T_o \\ T_o \\ T_o \\ T_o \end{bmatrix}
$$

(23)

3. Results and Discussion

With a domain for the analysis of axial depth z $=3.5\times10^{-6}$ meters and radius R= 25×10^{-6} meters and using the parameters in Table 1, using Alpha family of approximation the computed results are tabulated and shown graphically.

Table 1: Parameters used for the analysis

Parameters	Value
Gaussian Parameter a	120000^{-1} I/m
Ambient temperature T_o	298 K
Thermal conductivity k	52 W/(mK)
Reflectivity r_f	0.9
Density ρ	$7836 kg/m^3$
Absorption coefficient δ	6.16×10^7 I/m
Specific heat capacity C_p	330 J/kgK
Laser peak power intensity I_o	1×10^{13} W/m^2

Substituting the above parameters in Table 1 and the element size into (13), (14) and (15) to obtain the M, K and f element matrix for each of the elements making up the assembly as shown in Fig. 1 and Fig. 2 respectively.

For the Finite Element Analysis of the two dimensional time dependent partial differential equation, the solution comprises of two parts viz the semi discrete spatial approximation and the time approximation. For the semi discrete spatial approximation, uniform rectangular Lagrange interpolation functions were used to obtain the finite element model. Due to the rapid heating process, time spent during change of state (solid and liquid state) of the steel was assumed to be negligible and an average value of thermal conductivity k and specific heat capacity c_p was used for both states. Alpha α family of Approximation was used in the time analysis and the time step used was made as small as possible to improve the accuracy of the results. The accuracy of the method used in our analysis depends on the mesh discretization for the spatial approximation, and also the time step used for the time approximation. Highly accurate results are gotten from discretization with larger number of elements and smaller time step. To achieve this discretization a Finite Element Computer Programme is usually necessary. Table 2 and Table 3 shows the results of our computation of temperature values for 6 nano seconds using a discretization of 100 rectangular elements and 200 Triangular elements respectively. However with the computer programme developed we went further to discretized the domain using 2000 rectangular elements and 4000 triangular elements and the results were plotted alongside

the results of [14] in Fig. 3 to 18. Fig. 3 to Fig. 10 shows comparison of temperature distribution along the *z*-axes at some specified radial positions inside the substrate material for four different heating periods Fig. 11 to Fig. 18shows comparison of temperature distribution along the r-axes at some specified axial positions inside the substrate material for four different heating periods. From the Figures, the temperature values increases as the time of irradiation is increased, but at relatively high distance away from the surface (at depth close to 3.5μm and radius close to 25μm) the temperature variation with time is minimal as it is almost constant and this conforms to the boundary conditions of (5) and (6). At early heating periods of about 6ns, evaporation of the surface in the region of the irradiated spot centre begins and as the time period progresses, the cavity is formed in the surface vicinity of the substrate material. This is due to the laser power intensity distribution across the irradiated spot, which is Gaussian and energy absorbed from the irradiated field is unidirectional and along the axial direction. This in turn results in higher temperature gradients in the axial direction than that of the radial direction. As the depth below the surface increases towards the solid bulk, temperature decay becomes gradual. This occurs because of the energy balance attained between the internal energy gain from the irradiated field and diffusional energy transfer to solid bulk from the surface region [14].

For the laser model equation analyzed in (1), it was assumed that the thermal conductivity k and specific heat capacity c_p are constant and do not depend on the temperature of the irradiated material, but in reality it varies as the temperature increases as well as during phase change as the material changes from solid to liquid and then to vapor. However, these variations were not incorporated into the solution. Again it was assumed that the substrate material has sharp melting and boiling temperatures of 1880ºC and 3030ºC respectively, but during the laser heating, phase-change occurs.

Table 2: *Temperature values in Kelvin after 6 nano seconds using 100 rectangular element mesh*

Axial Depth (micro meters)	Radius (micro meters)										
	0.00	2.50	5.00	7.50	10.00	12.50	15.00	17.50	20.00	22.50	25.00
3.50	298.00	298.00	298.00	298.00	298.00	298.00	298.00	298.00	298.00	298.00	298.00
3.15	298.01	298.00	298.00	298.00	298.00	298.00	298.00	298.00	298.00	298.00	298.00
2.80	297.98	297.98	297.99	297.99	298.00	298.00	298.00	298.00	298.00	298.00	298.00
2.45	297.97	297.97	297.98	297.99	297.99	298.00	298.00	298.00	298.00	298.00	298.00
2.10	298.52	298.47	298.36	298.23	298.12	298.05	298.02	298.01	298.00	298.00	298.00
1.75	297.33	297.40	297.54	297.71	297.85	297.93	297.98	297.99	298.00	298.00	298.00
1.40	285.65	286.87	289.54	292.67	295.20	296.78	297.56	297.87	297.97	297.99	298.00
1.05	323.38	320.86	315.39	308.98	303.78	300.53	298.92	298.28	298.07	298.02	298.00
0.70	825.21	773.30	659.12	525.71	417.45	350.08	316.87	303.68	299.42	298.31	298.00
0.35	2875.80	2622.80	2063.50	1410.40	880.92	551.81	389.83	325.61	304.88	299.49	298.00
0.00	7595.10	6881.90	5295.00	3443.60	1944.40	1013.80	556.52	375.57	317.28	302.18	298.00

Table 3: *Temperature values in Kelvin after 6 nano seconds using 200 triangular element mesh*

| Axial Depth (micro meters)	Radius (micro meters)										
	0.00	2.50	5.00	7.50	10.00	12.50	15.00	17.50	20.00	22.50	25.00
3.50	298.00	298.00	298.00	298.00	298.00	298.00	298.00	298.00	298.00	298.00	298.00
3.15	298.07	297.80	298.22	298.16	297.80	297.90	298.00	298.03	298.03	298.01	298.00
2.80	298.41	297.21	298.23	298.76	297.93	297.75	297.84	297.94	298.01	298.03	298.00
2.45	299.84	295.80	297.14	299.64	298.84	298.10	297.82	297.79	297.88	297.96	298.00
2.10	305.71	293.65	292.45	298.65	300.02	299.46	298.67	298.11	297.92	297.91	298.00
1.75	328.96	296.58	281.89	289.96	296.55	299.27	299.66	299.03	298.43	298.11	298.00
1.40	414.59	336.76	280.54	273.29	281.41	290.23	295.86	298.01	298.36	298.23	298.00
1.05	698.48	531.72	380.85	303.26	278.51	278.86	286.91	293.35	296.52	297.66	298.00
0.70	1518.90	1198.90	873.61	594.65	419.58	333.32	302.82	296.35	296.58	297.40	298.00
0.35	3532.00	2969.80	2348.90	1592.20	982.21	599.38	408.44	331.56	306.44	299.72	298.00
0.00	3696.90	4128.50	3462.00	2384.40	1440.50	819.70	497.06	361.49	314.93	301.81	298.00
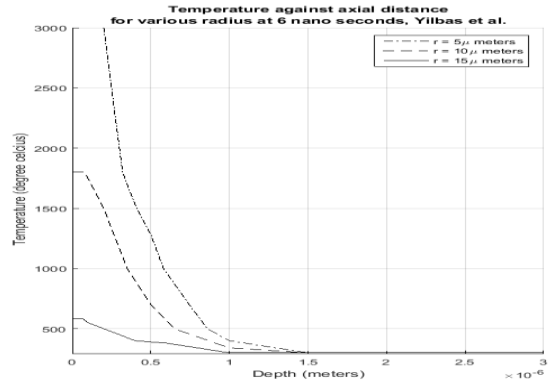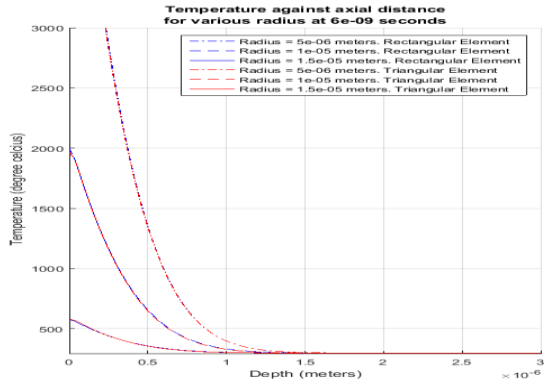
***Fig. 3:** Temperature against axial distance at time 6 nano seconds (Comparison between this work and that of Yilbas et al. [13-15])*
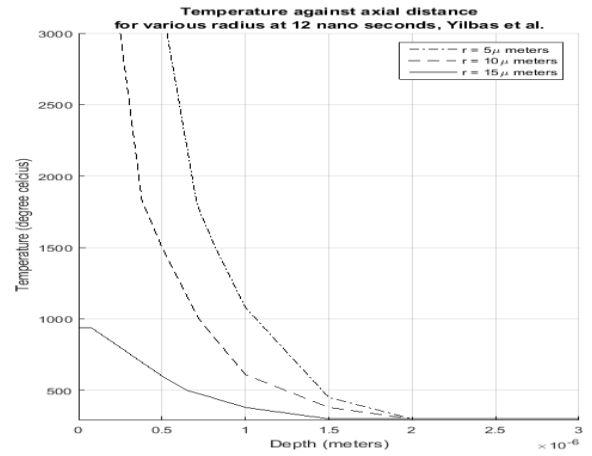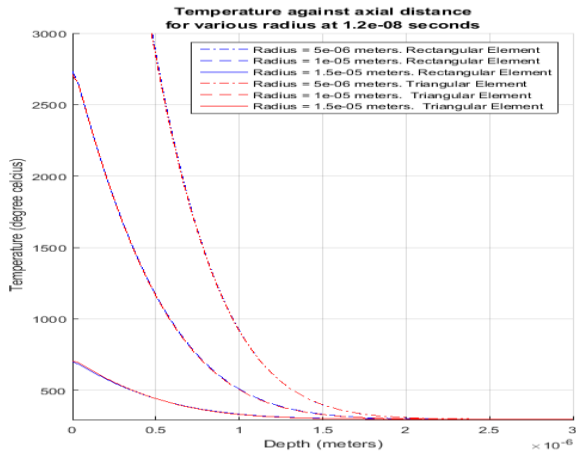

***Fig. 4:** Temperature against axial distance at time 12 nano seconds (Comparison between this work and that of Yilbas et al. [13-15])*
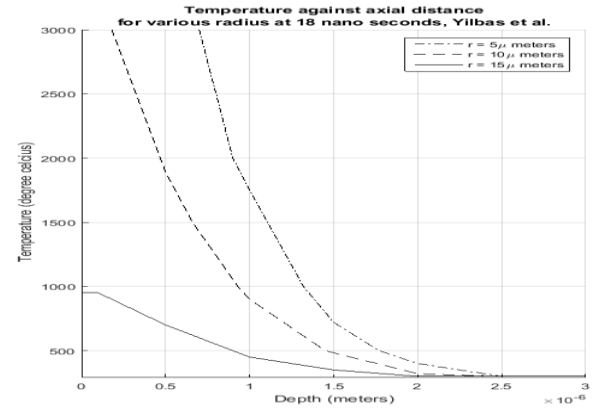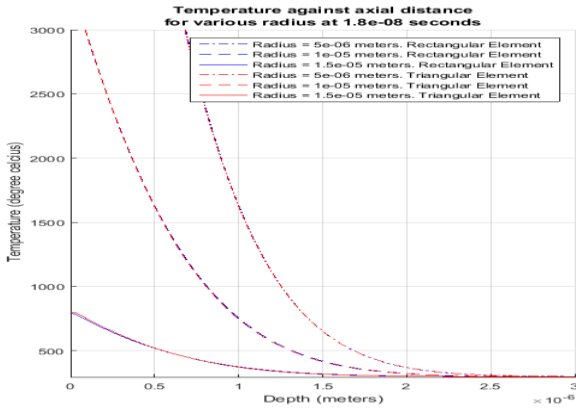

***Fig. 5:** Temperature against axial distance at time 18 nano seconds (Comparison between this work and that of Yilbas et al. [13-15])*
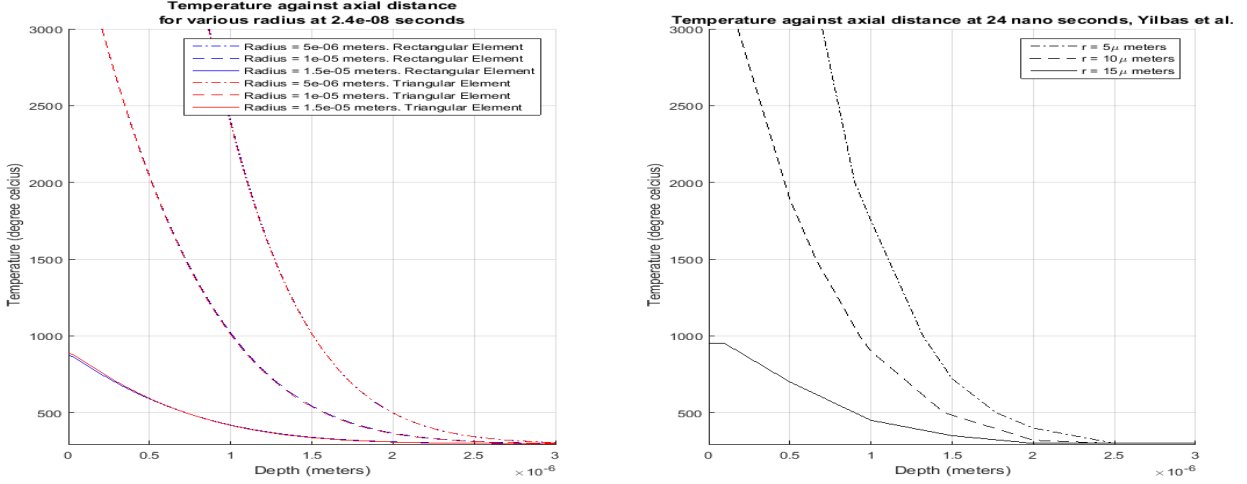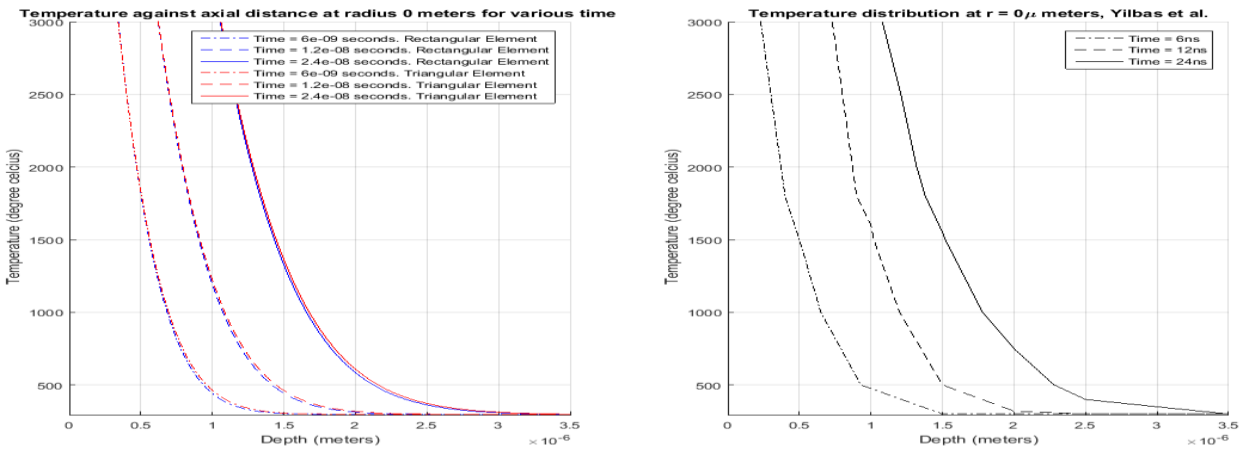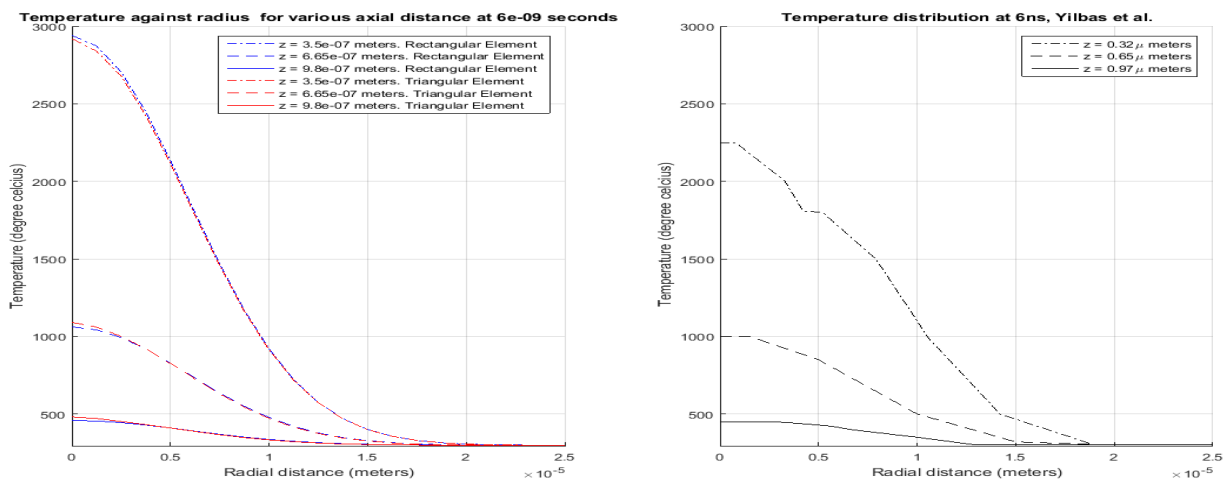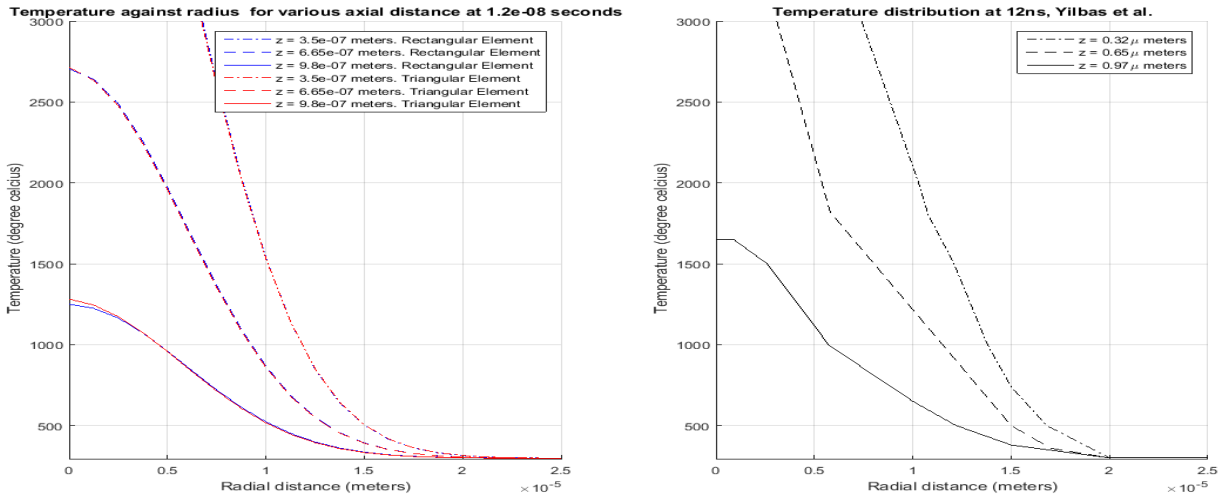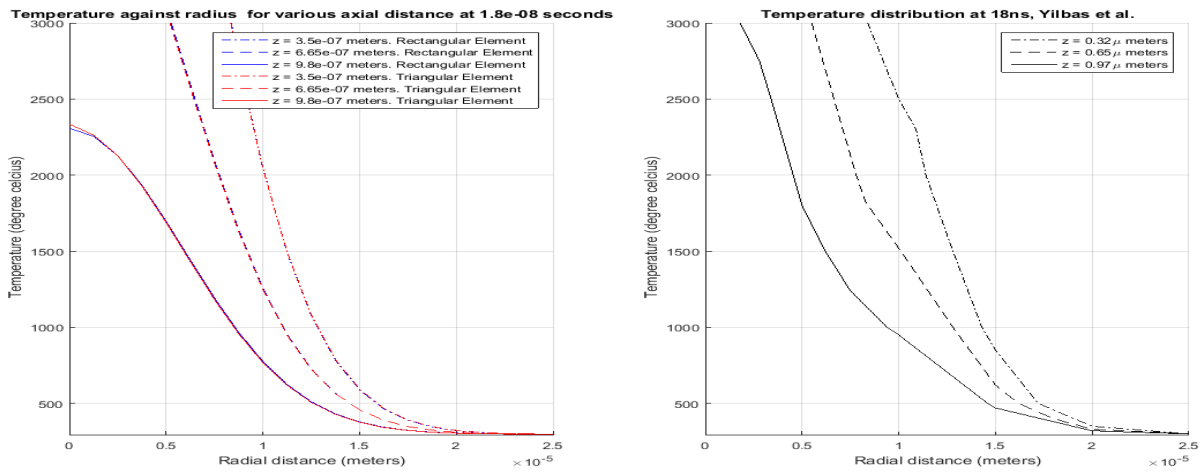
Fig. 6: *Temperature against axial distance at time 24 nano seconds (Comparison between this work and that of Yilbas et al. [13-15])*

Fig. 7: *Temperature against axial distance for radius 0 micro meters (Comparison between this work and that of Yilbas et al [13-15])*
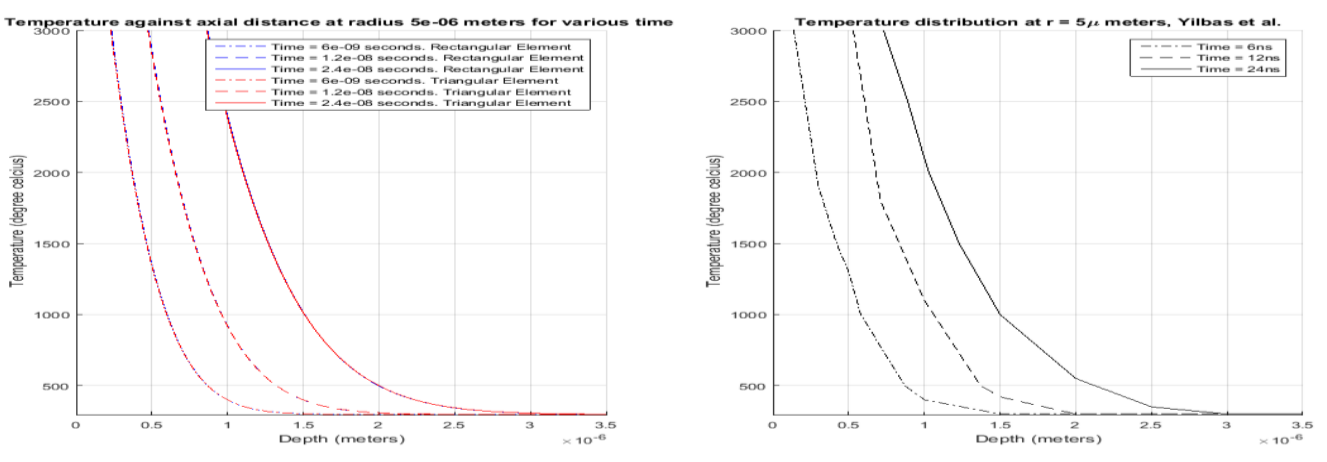
Fig. 8: *Temperature against axial distance for radius 5 micro meters (Comparison between this work and that of Yilbas et al [13-15])*
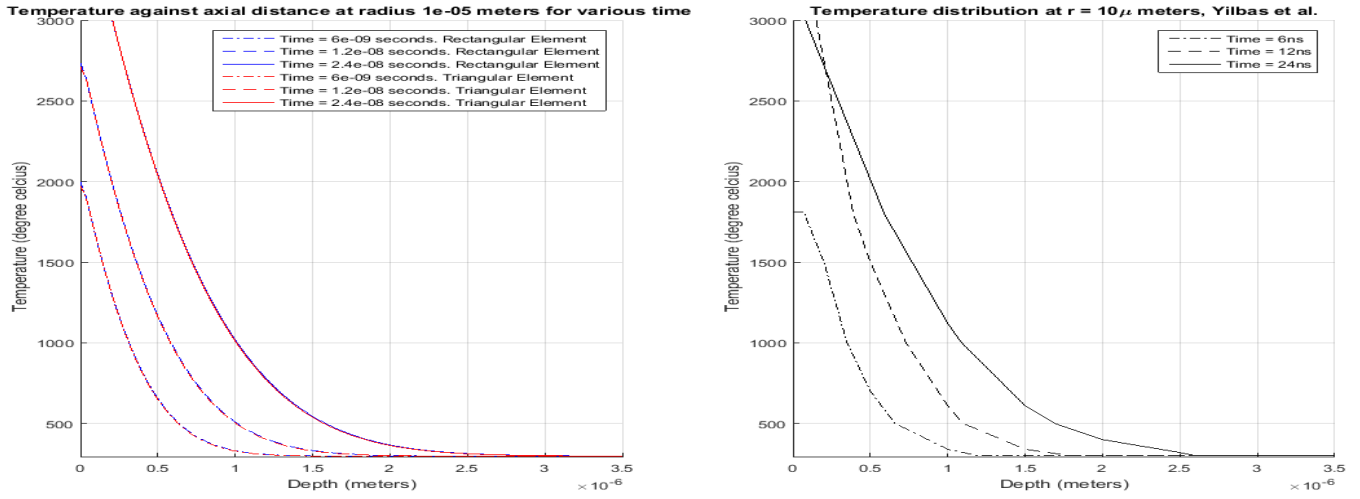
Fig. 9 *Temperature against axial distance for radius 10 micro meters (Comparison between this work and that of Yilbas et al [13-15])*
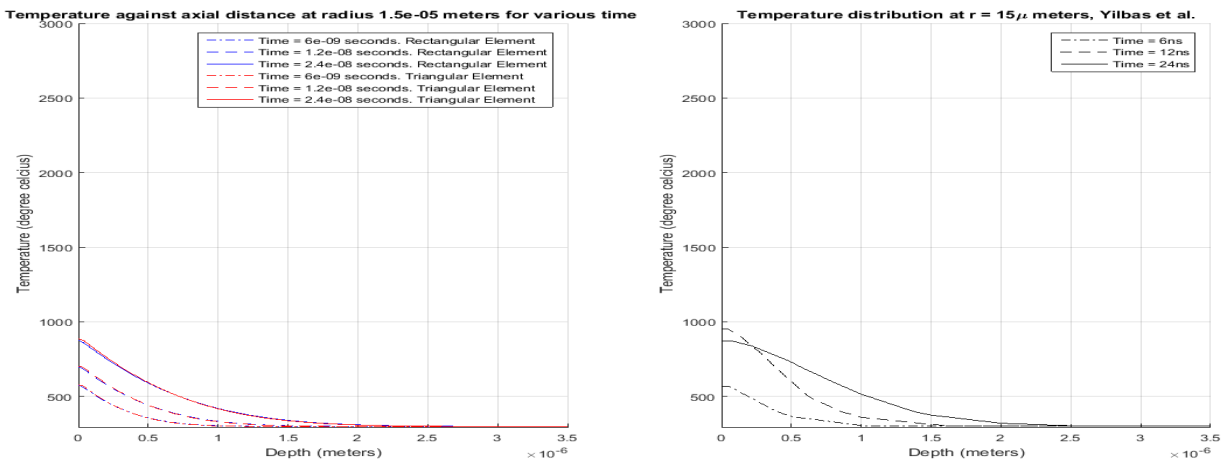
Fig. 10: *Temperature against axial distance for radius 15 micro meters (Comparison between this work and that of Yilbas et al[13-15])*

Fig. 11: *Temperature against radius at time 6 nano seconds (Comparison between this work and that of Yilbas et al. [13-15])*
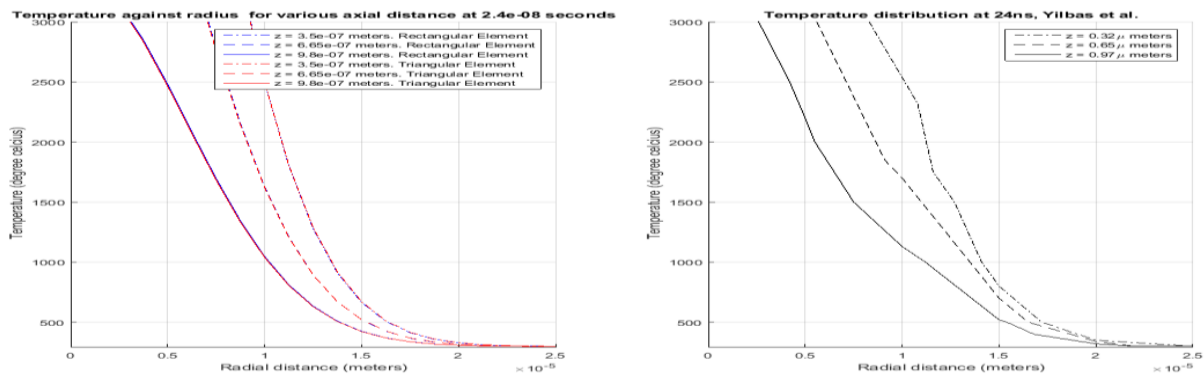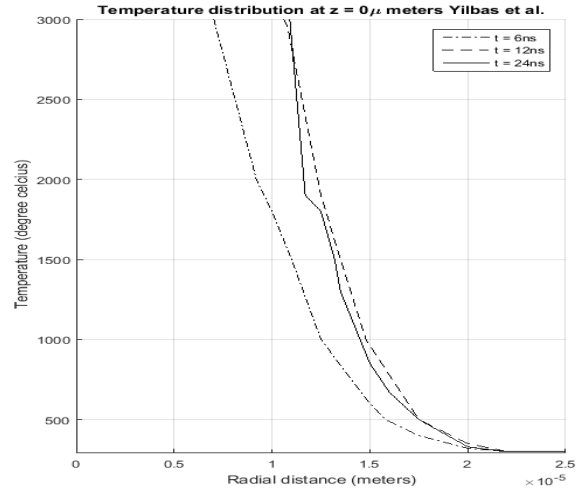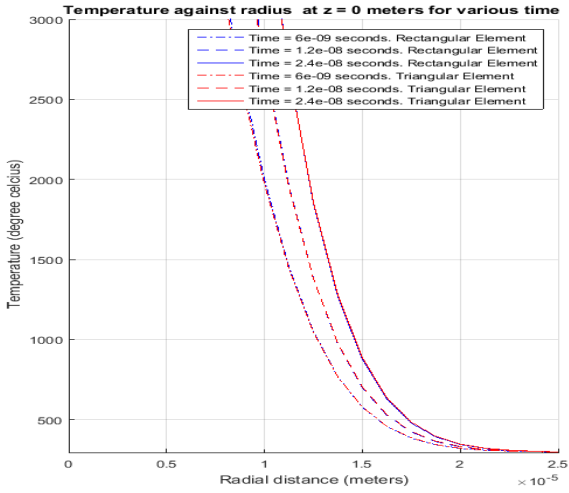
117

Fig. 12: *Temperature against radius at time 12 nano seconds (Comparison between this work and that of Yilbas et al. [13-15])*

Fig. 13: *Temperature against radius at time 18 nano seconds. (Comparison between this work and that of Yilbas et al. [13-15])*

Fig. 14: *Temperature against radius at time 24 nano seconds (Comparison between this work and that of Yilbas et al. [13-15])*

Fig. 15: *Temperature against radius at axial distance of 0 micro meters. (Comparison between this work and that of Yilbas et al. [13-15])*
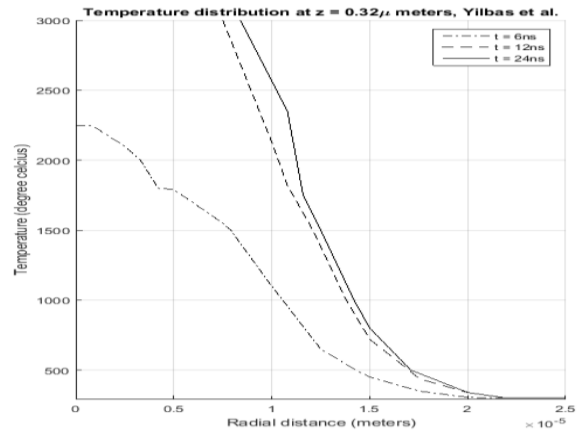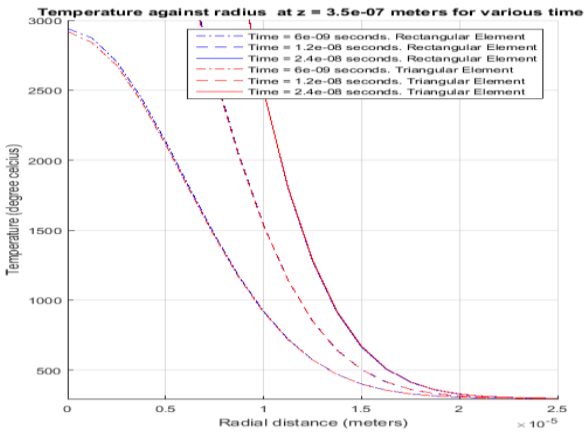

Fig. 16: *Temperature against radius at axial distance of 0.35 micro meters (Comparison between this work and that of Yilbas et al. [13-15])*
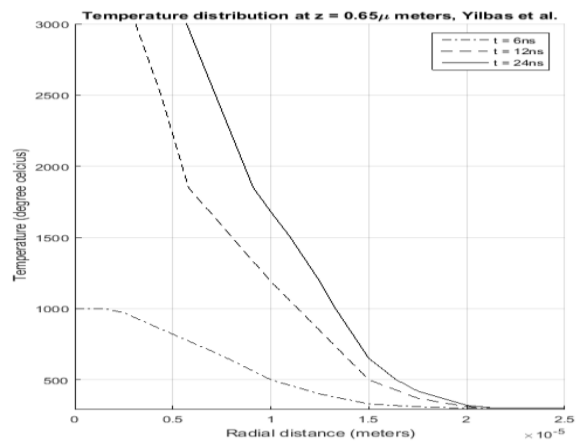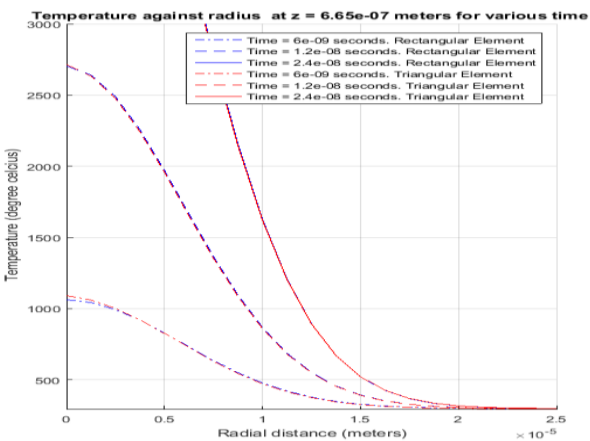

Fig. 17: *Temperature against radius at axial distance of 0.665 micro meters. (Comparison between this work and that of Yilbas et al. [13-15])*
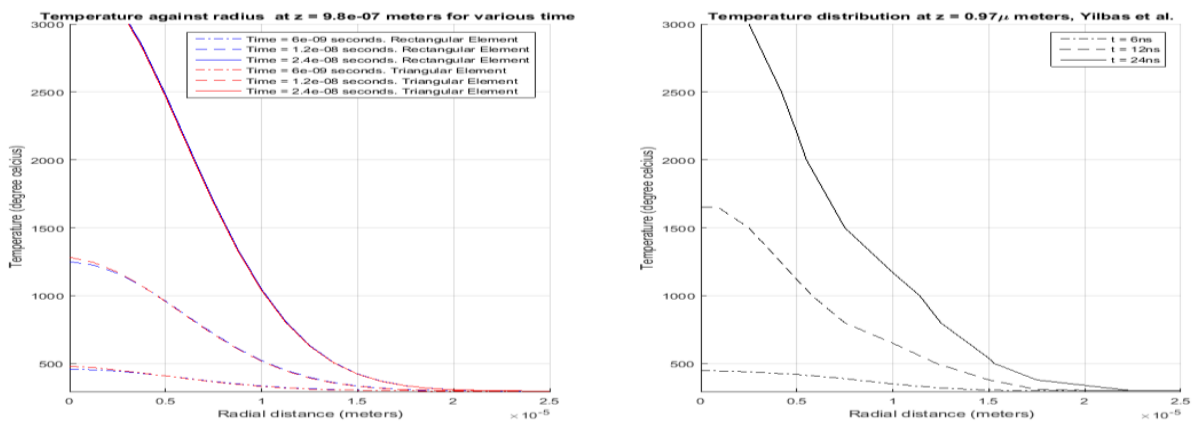
Fig. 18: *Temperature against radius at axial distance of 0.98 micro meters(Comparison between this work and that of Yilbas et al.[13-15])*

To accommodate the phase change process, a mushy zone is created and it should be considered if actual heating model is to be fully considered. That is, the Laser heating equation should be modified. For the modification an energy (or enthalpy) method can be used. In the enthalpy method, the governing equation of energy transport can be written in terms of an enthalpy equation. Once the phase change initiates, a mushy zone (partially solid and partially liquid or partially liquid and partially vapor) can be generated across the interface where the phase change occurs. During the phase change process, the temperature of the substrate material remains the same, but its enthalpy changes in this region. This can be formulated after considering the energy balance in the mushy zone, [14].

Conclusion

The Laser heating equation (1) has been successfully solved using Finite Element Method a numerical method as against the analytical. It can therefore be concluded that the Finite Element Method is capable of adequately and accurately predicting the temperature distribution in the irradiated material, With its accuracy increasing as we increase the number of Finite Elements discretization, Such that using a mesh discretization up to 2000 rectangular elements and 4000 triangular elements by the help of the MATLAB program developed we have results that were highly accurate as seen from the graphs. The Finite Element procedures used in the analysis can be applied to all similar Laser heat equations by simply substituting appropriate parameters and boundary conditions into the formulated coefficient matrix equation in the MATLAB Finite Element program developed.

References

[1] D S Burnett., *Finite Element Analysis, from Concept to Application.* Addison Wesley, New Jersey, 1987.
[2] J.N. Reddy, *An Introduction to the Finite Element Method.* Third ed. McGraw-Hill. 2006.
[3] J.A. Akpobi, and E.D., Akpobi. "A finite element analysis of the distribution of velocity in viscous incompressible fluids using the Lagrange interpolation function", *Journal of Applied Science*, vol.11, pp.31-38, 2007.
[4] J.A. Akpobi, and E.D., Akpobi. "Finite element solution of the Boussinesq wave equation", *Journal of the Nigeria association of Mathematical physics*, vol.11, pp. 223-228. 2007.
[5] H. Shokouhmand and S.M.A. Noori., "Finite element analysis of mixed convection heat transfer through a vertical wavy isothermal channel", *proceedings of the world congress on Engineering*, vol. 2, pp. 1415-1420, 2010.

[6] R. Rajamani, C. Srinivas, and K. N. Seetharamu, "Finite Element Analysis of convective Heat transfer in porous media", *International journal for Numerical Methods in Fluids*. Vol.11 (3), pp. 331-339, 1990.

[7] Johan Meijer,."Laser beam machining (LBM), state of the art and new opportunities", *Journal of Materials Processing Technolog* vol. 149 pp. 2–17, 2004.

[8] U. Paek, and F. P. Gagliano "Thermal analysis of laser drilling", *Journal of Quantum Electronics*, vol.8, pp.112-119, 1972.

[9] X.Liu, D. Du, and G. Mourou, " Laser ablation and micro machining with ultrashort laser pulses, Journal of Quantum Electron. Vol. 33, pp. 1706-1716, 1997.

[10] M. F. Modest and H. Abiakans, "Evaporative cutting of a semi-infinite body with a moving cw laser", *Journal of Heat Transfer*, vol. 108 pp. 602-607, 1988.

[11] P. S. Wei and J. Y. Ho, Energy consideration in high energy beam drilling, International Journal of Heat and Mass Transfer, vol. 33, pp. 2207-2217, 1990.

[12] S.Y. Bang and M. F. Modest, "Multiple reflection effects on evaporative cutting with a moving cw laser", *Journal of Heat Transfer*, vol. 113, pp. 663-669, 1991.

[13] B. S. Yilbas and I. Z. Naqvi, "Laser heating including the phase change process and thermal stress generation in relation to drilling", *Journal of Engineering Manufacture*, vol. 217(B) pp. 977-991, 2003.

[14] B. S. Yilbas, M. Saad, and S. Z. Shuja, "Laser pulse heating: modelling of cavity formation", *Journal of Mechanical Engineering Science*, vol. 221(C) pp. 307-328, 2006.

[15] B. S. Yilbas, "Analytical solution for time unsteady laser pulse heating of semi-infinite solid", *International journal of Mechanical Science*, vol. 39(6), pp. 671-682, 1997.